EXPLORING CLUSTER ELLIPTICAL GALAXIES AS COSMOLOGICAL STANDARD RODS[1,2]

Ralf Bender,[3] R. P. Saglia, Bodo Ziegler,[3] Paola Belloni,
Laura Greggio,[4] and Ulrich Hopp
Universitäts-Sternwarte, Scheinerstrasse 1, 81679 München, Germany

AND

Gustavo Bruzual
CIDA, Apartado Postal 264, Mérida 5101-A, Venezuela

ABSTRACT

We explore the possibility of calibrating massive cluster elliptical galaxies as cosmological standard rods using the fundamental plane relation combined with a correction for luminosity evolution. Although cluster ellipticals certainly formed in a complex way, their passive evolution out to redshifts of about 1 indicates that basically all major merging and accretion events took place at higher redshifts. Therefore, a calibration of their luminosity evolution can be attempted. We propose to use the Mg-σ relation for that purpose because it is independent of distance and cosmology. We discuss a variety of possible caveats, ranging from dynamical evolution to uncertainties in stellar population models and evolution corrections to the presence of age spread. Sources of major random and systematic errors are analyzed as well.

We apply the described procedure to nine elliptical galaxies in two clusters at $z = 0.375$ and derive constraints on the cosmological model. For the best-fitting Λ-free cosmological model we obtain $q_0 \approx 0.1$, with 90% confidence limits being $0 < q_0 < 0.7$ (the lower limit being due to the presence of matter in the universe). If the inflationary scenario applies (i.e., the universe has flat geometry), then, for the best-fitting model, matter and Λ contribute about equally to the critical cosmic density (i.e., $\Omega_m \approx \Omega_\Lambda \approx 0.5$). With 90% confidence, Ω_Λ should be smaller than 0.9.

Subject heading: cosmology: observations — galaxies: elliptical and lenticular, cD — galaxies: evolution — galaxies: formation

1. INTRODUCTION

A central issue of modern cosmology is the determination of the geometry of the universe or, equivalently, of its density parameter Ω and of the cosmological constant Λ. In recent years, several lines of argument indicate that Ω may be smaller than 1, and, therefore, the universe may be open and have negative curvature. On the other hand, if the inflationary scenario applies (see, e.g., Linde 1991), then the universe should have flat geometry, i.e., either the matter density has the critical value ($\Omega_m = 1$) or, if $\Omega_m < 1$, $\Omega_m + \Omega_\Lambda = 1$ with $\Omega_\Lambda = \Lambda/(3H_0^2)$. In the latter case, a nonzero cosmological constant is needed, which may have interesting consequences for the cosmological deceleration parameter $q_0 = \Omega_m/2 - \Omega_\Lambda$, i.e., q_0 may be negative.

Most methods to determine the deceleration parameter q_0 directly rely on the variation of the *apparent* sizes or brightnesses of standard objects with redshift (Sandage 1995). So far, all measurements were inconclusive, because all objects that were bright or large enough to be potential standard rods or candles (e.g., galaxies or clusters of galaxies) show significant evolution with redshift. In fact, until now most attempts to measure q_0 were better tests for galaxy and cluster evolution than for the cosmological model. Only recently, Type Ia supernovae (SNe Ia), which may be true standard candles, have raised hopes for tighter constraints on q_0 (e.g., Goobar & Perlmutter 1995; Leibundgut 1996). The ongoing SN Ia programs promise indeed to provide significant constraints on q_0 (e.g., Perlmutter et al. 1997), once enough SNe Ia have been found at intermediate redshifts and all observational caveats have been understood.

In this paper we want to explore whether luminous cluster ellipticals can be calibrated as cosmological standard rods. Although it is almost certain that luminous elliptical galaxies have experienced a complex formation history (with events ranging from accretion of satellite galaxies to violent similar-mass mergers (see, e.g., Bender 1990; Schweizer 1990), most of these events took place early in their evolution. This follows both from the homogeneous properties of local cluster ellipticals (Dressler et al. 1987; Bower, Lucey, & Ellis 1992; Bender, Burstein, & Faber 1993; Renzini & Ciotti 1993) and from the very small redshift evolution of luminosities (Glazebrook et al. 1995; Lilly et al. 1995), colors (Stanford, Eisenhardt, & Dickinson 1998; Ellis et al. 1997), and spectral indices (Bender, Ziegler, & Bruzual 1996). Furthermore, the redshift evolution of the fundamental plane relation of elliptical galaxies (Djorgovski & Davis 1987; Faber et al. 1987; Bender, Burstein, & Faber 1992) has also been found to be consistent with passive evolution of the stellar populations in ellipticals (van Dokkum & Franx 1996; Kelson et al. 1997). Basically

passive evolution of cluster ellipticals is expected even in the most rapidly evolving standard cold dark matter model, where neither significant star formation nor accretion processes take place at $z < 0.5$ (Kauffmann 1996). The star formation activity observed in distant clusters of galaxies seems to be confined to blue infalling and/or harassed disk galaxies (Oemler, Dressler, & Butcher 1997; Moore, Lake, & Katz 1998 Balogh et al. 1997), which may turn into intermediate-luminosity S0 today but are unlikely to alter the population of massive cluster ellipticals at a significant level.

Because massive cluster ellipticals evolve only passively up to redshifts $z = 0.5, \ldots, 1$, one can attempt to calibrate them as cosmological standard rods. The method proposed here is based on the fundamental plane (FP) relation of elliptical galaxies, which allows us to derive accurate radii from their velocity dispersions and surface brightnesses, combined with a correction for luminosity evolution obtained from the Mg-σ test (Bender et al. 1996). We give a first application of this method by deriving constraints on q_0 from nine ellipticals in two clusters at $z = 0.375$. In § 2 we present the method, and in § 3 we discuss possible caveats. In § 4 observations and data analysis are described, the results of which are presented in § 5. Conclusions are drawn in § 6.

2. CALIBRATING ELLIPTICAL GALAXIES AS STANDARD RODS

The FP describes the observed tight scaling relation between effective radius (R_e), mean effective surface brightness ($\langle SB \rangle_e$), and velocity dispersion (σ) of cluster ellipticals:

$$\log R_e = 1.25 \log \sigma + 0.32 \langle SB \rangle_e - 8.895 , \qquad (1)$$

with R_e in kiloparsecs, σ in kilometers per second, and $\langle SB \rangle_e$ in the B band. The constant -8.895 was derived from the Coma Cluster elliptical galaxies with a Hubble constant of $H_0 = 50$ km s^{-1} Mpc^{-1}, the error in the constant is about 0.01 (see below). The FP allows us to predict the effective radii R_e of elliptical galaxies with better than 15% accuracy from their velocity dispersions and surface brightnesses, i.e., a distance-dependent quantity (R_e) can be estimated from two distance-independent quantities (σ, $\langle SB \rangle_e$). If a large enough number of ellipticals are measured per cluster, then the distance to the corresponding cluster can be determined with significantly better than 5% accuracy because otherwise the observed peculiar velocities of clusters would be much larger (e.g., Burstein 1989; Jørgensen, Franx, & Kjærgaard 1996).

As argued in § 1, we have strong evidence that massive ellipticals in rich clusters evolve only passively between now and at least $z \approx 0.5$. Passive evolution of the stellar population can be accurately measured with the Mg-σ relation, which is independent of q_0 and H_0 (Bender et al. 1996) and is within current limits the same for clusters of similar richness/velocity dispersion (Jørgensen 1997; see also below). In local cluster ellipticals, the Mg$_b$ absorption is tightly coupled to the velocity dispersion σ of the galaxy, constraining the scatter in age and metallicity at a given σ to be smaller than 15%. Therefore, in the case of passive evolution, Mg$_b$ decreases with redshift only because the age of the population decreases. One can use population synthesis models to translate the observed Mg$_b$ weakening into an estimate of the B-band luminosity evolution. Based on
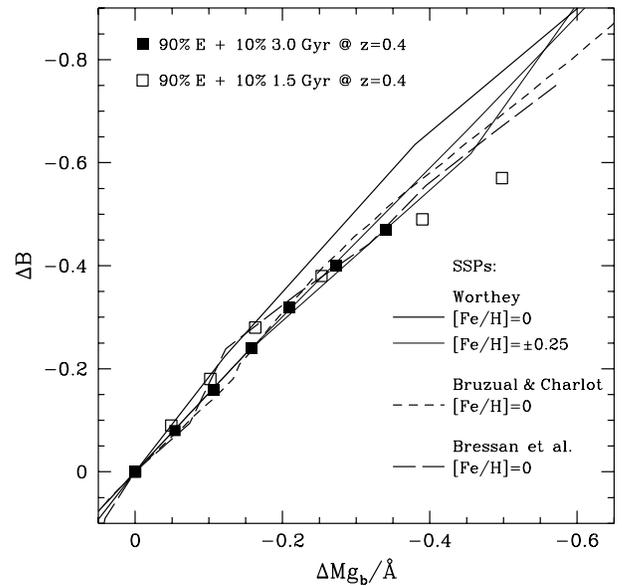

FIG. 1.—Differential relation between Mg$_b$ absorption and B-band luminosity as a function of age for different metallicities. Lines for different metallicities were normalized to the same B-band luminosity at an age of 12 Gyr and refer to simple stellar populations. Composite stellar populations are indicated with open and filled squares. The open (filled) squares trace the differential evolution of a single galaxy that consists of 90% of an old population, designated E, to which a starburst added a mass of 10% 1.5 Gyr (3 Gyr) before observation at $z = 0.4$.

models by Worthey (1994), Bruzual & Charlot (1998), and Bressan, Chiosi, & Tantalo (1996), we obtain consistently $\Delta B = 1.4 \Delta$Mg$_b$ for a Salpeter initial mass function, and metallicities between $\frac{1}{3}$ and 3 times solar and ages between 3 and 15 Gyr (see Fig. 1). The slope of 1.4 shows no dependence (within 0.1) on evolutionary tracks and other differences in the synthesis models, which demonstrates that this differential comparison of Mg$_b$ and B-band evolution is quite robust (see also § 3).

3. CAVEATS

Obviously, a number of caveats have to be addressed at this point. Most of them need further checking before ellipticals can reliably serve as standard rods. However, the influence of all these effects is rather small, and there is justified hope that they may be controlled better in the future.

1. *Dynamical evolution.*—We now have very good evidence that dynamical evolution will not alter the FP at a detectable level. There are two simple observational arguments. First, different types of objects, like anisotropic ellipticals, rotationally flattened ellipticals, and S0 galaxies, show no significant offsets from the mean FP relation. This means that objects of very different internal structure and dynamics and very different formation/evolution histories are indistinguishable in the edge-on view of the FP, implying that changes in the dynamical structure transforming objects from one type to another will not affect the FP relation. Second, the successful use of the FP to derive peculiar motions from clusters and groups of galaxies of different richness and internal evolution (Burstein, Faber, & Dressler 1990) indicates that environment and interaction can alter the FP parameters on the few percent level at most. Finally,

recent numerical simulations show that dissipationless merging of objects within the FP produces objects that are again in the plane (Capelato, de Carvalho, & Carlberg 1995).

2. *Dependence on environment* (i.e., systematic differences between the FP and Mg-σ relations of different clusters).—At present, the small observed peculiar velocities of clusters (e.g., Burstein 1989; Jørgensen, Franx, & Kjærgaard 1996) imply that the systematic variation of the FP zero point from cluster to cluster must be significantly smaller than 5%. For the Mg-σ relation a weak dependence on cluster velocity dispersion or richness has been observed (Jørgensen 1997; but see Colless et al. 1998) In any case, there is no evidence that, at a given richness, the zero point of the Mg_b-σ relation varies by more than 0.08 Å. Furthermore, the effects of different zero points can be minimized by observing a large enough sample of ellipticals in different clusters.

3. *Sample selection effects.*—We estimated the combined biasing effect of the sample size, sample selection, and allowed range of the FP parameters by means of Monte Carlo simulations following Saglia et al. (1997b). We find that the systematic bias of the FP zero point is smaller than the random variation estimated in Table 1, for the range of FP coefficients given by Jørgensen et al. (1996). A large complete sample of distant cluster ellipticals can minimize selection effects.

4. *Dust absorption.*—Dust absorption can be estimated by comparing colors and line-strength indices. We could rule out a significant presence of dust in the $z = 0.375$ ellipticals by checking the relation between their rest-frame $B - V$ color and their Mg_b values, finding that it is consistent with the local $(B - V)$–Mg_b relation (e.g., Bender et al. 1993) and population synthesis models (Worthey 1994).

5. *Population synthesis models.*—At present, population synthesis models (e.g., Worthey 1994; Bruzual & Charlot 1998; Bressan et al. 1996) do not always give a consistent interpretation of ages and metallicities of stellar populations. Close inspection shows that the differences mostly arise because of different zero points in the modeled magnitudes, colors, and line strengths for a given age-metallicity combination. However, the different models agree very well with respect to *differential* relations. For example, dMg_b/dB as a function of age is virtually the same for all models, despite different stellar evolution tracks and numerical codes (see Fig. 1). At present, the biggest uncertainty with respect to the method discussed here stems from the fact that all synthesis codes rely on the same set of fitting functions for the line indices, introduced by Gorgas et al. (1993)

and revised by Worthey (1994). These reproduce the Mg indices of G and K stars as a function of temperature, gravity, and metallicity in an excellent manner, but only for stars with solar abundance ratios, while massive ellipticals are overabundant in Mg relative to Fe. It is plausible that the *differential* temperature dependence of the Mg_b index is not very sensitive to this effect, but further checking is needed.

6. *Initial mass function.*—The relation between time evolution in the B band and Mg_b is dependent on the exponent x of the initial mass function (IMF). From models of Bruzual & Charlot (1998) we find $\Delta B = 1.4[1 - 0.3(x - x_s)]\Delta Mg_b$, where the subscript s indicates the Salpeter exponent ($x_s = 1.35$). At present, there is neither evidence nor a convincing physical argument for an IMF slope much different from Salpeter's for the metallicities around solar and for the mass range concerned (between 0.8 and 1.2 $M_\odot$). Still, this is a key assumption for the method to work.

7. *Effects of mixed populations.*—We performed tests with varying fractions of intermediate-age populations superposed on an old population, all constrained in such a way that the objects at $z = 0.375$ would *not* be regarded as of $E + A$ type from spectral characteristics (Dressler & Gunn 1983). For plausible population mixes, the uncertainty in the evolution correction is smaller than 0.1 mag in the B band. Figure 1 shows two examples for the Mg_b versus B-band evolution of mixed populations. One experienced a 10% starburst 3 Gyr, the other 1.5 Gyr before the redshift of observation ($z = 0.4$). In the second case a significant curvature is present in the Mg_b-B relation. This indicates that evolution effects due to mixed populations with $\Delta B < -0.6$ mag are more difficult to correct reliably. However, note that in case of massive ellipticals it is very difficult to add 10% of young stars over a short period because the gas content of most objects that can be accreted is too small relative to the total mass of the elliptical.

4. A FIRST APPLICATION: OBSERVATIONS AND DATA ANALYSIS

We analyzed a sample of nine elliptical galaxies in the clusters Abell 370 and MS 1512 + 36 at $z = 0.375$. Abell 370 is of richness similar to that of the Coma Cluster, which serves as our local calibrator; MS 1512 + 36 is less rich.

Spectroscopic data were obtained at the Calar Alto 3.5 m telescope and the New Technology Telescope (NTT) at ESO. Details of the spectroscopic observations and data analysis can be found in Ziegler & Bender (1997). The largest uncertainty in the obtained velocity dispersions and Mg_b indices comes from the applied aperture corrections

TABLE 1
BUDGET OF MAJOR ERRORS FOR $z = 0.375$ CLUSTERS RELATIVE TO COMA CLUSTER

Source of Error	Error for Single Object	Error of Mean for 9 Objects
Photometric ZP	$\Delta SB_e \approx 0.020$	≈ 0.020
Transformation to rest frame	$\Delta SB_e \approx 0.030$	≈ 0.020
Reddening correction	$\Delta SB_e \approx 0.020$	≈ 0.020
Kormendy product $R_e I_e^{-0.8}$	$\Delta SB_e \approx 0.030$	≈ 0.011
Evolution correction	$\Delta SB_e \approx 0.180$	≈ 0.064
Velocity dispersion	$\Delta \log \sigma \approx 0.040$	≈ 0.014
Physical scatter in FP	$\Delta FP \approx 0.040$	≈ 0.014
Total error	$\Delta FP \approx 0.087$	≈ 0.032

NOTE.—With FP = $1.25 \log \sigma + 0.32\langle SB \rangle_e - 8.895$ and $\langle SB \rangle_e = -2.5 \log I_e + $ constant. For a brief discussion of the error in the Kormendy product see text. Note that the error of the mean is in some cases larger than the expected statistical error because of systematic effects.

necessary to compare local and distant ellipticals. However, the errors from aperture corrections can be expected to become smaller in the near future because better data for nearby ellipticals will allow us to integrate over apertures large enough for direct comparison with distant ellipticals, and spatial resolution will also improve for distant ellipticals as a result of the use of large telescopes. The spectroscopic parameters for the local comparison sample were taken from Faber et al. (1989). At present, there still exists some uncertainty in the parameters of the low-redshift Mg_b-σ relation (Dressler et al. 1987; see Fig. 2) because the Mg_2 values for Coma and Virgo ellipticals have to be transformed to Mg_b values. However, this uncertainty is not crucial at the present stage of analysis and will be reduced by future measurements. We used the relation $Mg_b = 15.0$ Mg_2; see Ziegler & Bender (1997).

Accurate radii and surface brightnesses for the distant ellipticals were obtained with the Hubble Space Telescope (HST) and the refurbished Wide Field and Planetary Camera (WFPC2). The structural parameters R_e and $\langle SB \rangle_e$ in the F675W filter were derived using the two-component fitting algorithm developed by Saglia et al. (1997a), with HST point-spread function convolution tables. Ground-based imaging at the ESO NTT and the Calar Alto 2.2 m telescope in several colors (Ziegler 1998) complemented the HST imaging and allowed an accurate transformation to rest-frame colors using models of Bruzual & Charlot (1998). Surface brightnesses were transformed to the rest-frame B band, corrected for cosmological dimming $[(1 + z)^4]$ and for passive evolution using the Mg_b-σ relation described

above. Galactic extinction was corrected using extinctions of Burstein & Heiles (1984), kindly provided by D. Burstein.

The photometric parameters of the local comparison sample of Coma galaxies (Saglia, Bender, & Dressler 1993) were rederived with the same procedure that was used for the $z = 0.375$ objects. The B-band photometric zero points were improved using aperture photometry from Longo, de Vaucouleurs, & Corwin (1983) and Jørgensen, Franx, & Kjærgaard (1995), reducing the rms scatter about the Coma FP to about 10% in the effective radius (see Fig. 3). We applied K-corrections and corrections for Galactic extinction as in Faber et al. (1989), plus the correction for the cosmological dimming of surface brightness. Since the $z = 0.375$ ellipticals are about a factor of 10 more distant than the Coma galaxies, the factor of 10 better sampling and smaller PSF of HST relative to the ground-based imaging of Coma corresponds to a perfectly matched instrumental setup.

4.1. Error Analysis

An account of the major sources of error is given in Table 1. The dominant error is due to the correction for luminosity evolution. This error is partly random and partly systematic. For the rather few objects we consider here, the
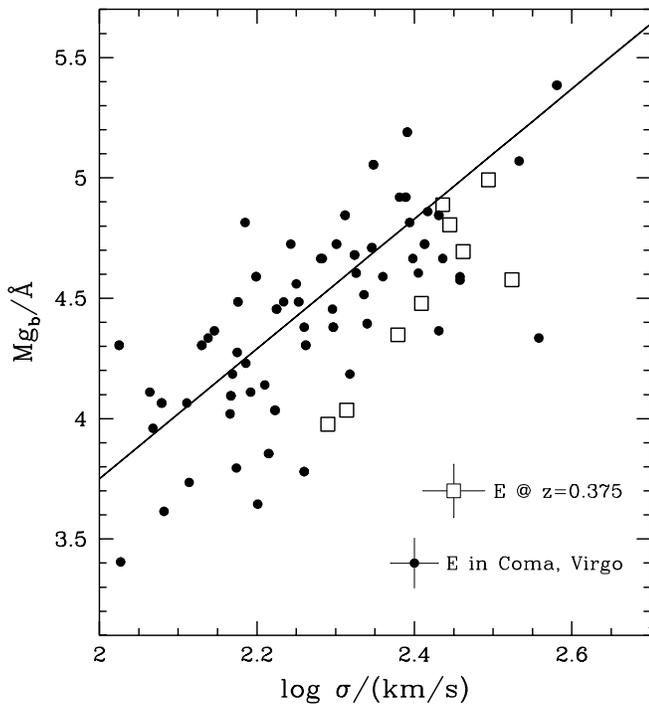

FIG. 2.—The Mg_b-σ relation for elliptical galaxies in the Coma and Virgo clusters (filled circles) and for elliptical galaxies in Abell 370 and MS 1512+36, both at $z = 0.375$ (open squares). All measurements have been brought to consistent aperture sizes. Typical error bars are given at the lower right. The best fit to the Coma data is $Mg_b = 2.7 \log \sigma - 1.65$, with σ in kilometers per second. The lower Mg_b of the distant ellipticals at a given σ is due to the (passive) evolution of their stellar populations with redshift.
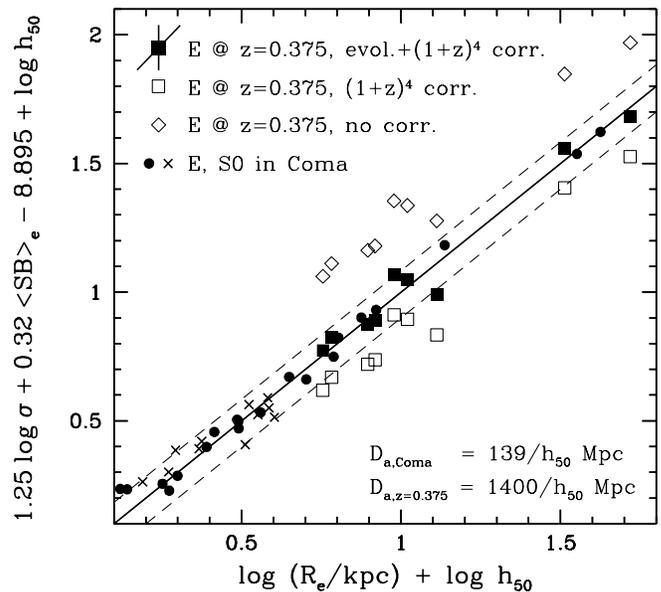

FIG. 3.—The fundamental plane of elliptical and S0 galaxies. Small filled circles and small crosses denote elliptical galaxies and S0 galaxies in the Coma Cluster with velocity dispersions $\sigma > 120$ km s^{-1}, effective radii R_e in kiloparsecs, and effective surface brightnesses $\langle SB \rangle_e$ in the B band, h_{50} is the Hubble constant in units of 50 km s^{-1} Mpc^{-1}. The typical measurement errors for the Coma objects are somewhat smaller than the scatter indicates. The large open diamonds show elliptical galaxies in Abell 370 and MS 1512+36, both at a redshift of $z = 0.375$, as observed and transformed to the B-band rest frame. The large open squares show the $z = 0.375$ ellipticals after surface brightness has been corrected for cosmological $(1 + z)^4$ dimming. The large filled squares represent the redshifted ellipticals after a further correction for mean luminosity evolution has been applied. The correction was derived from the offset in the Mg-σ relations between the distant and local ellipticals (see Fig. 2). A typical error bar is shown for the $z = 0.375$ ellipticals at the upper left. The FP relations match for an angular distance to Coma of 139 Mpc h_{50}^{-1} and an angular distance of 1400 Mpc h_{50}^{-1} to Abell 370 and MS 1512+36 at $z = 0.375$. The upper and lower dashed lines show the mean FP relations of the $z = 0.375$ objects if they were at a distance of 1100 Mpc h_{50}^{-1} or 1700 Mpc h_{50}^{-1}, respectively.

random error is still dominating. Note that because of error coupling in the Kormendy relation $R_e \propto I_e^{0.8}$ (I_e = surface brightness in linear flux units), the error in $R_e I_e^{-0.8}$ is much smaller than in each of R_e and I_e separately (Kormendy 1977; Hamabe & Kormendy 1987).

The fact that the scatter of the $z = 0.375$ ellipticals around the FP is somewhat smaller (only 15%) than we expect from the error estimate ($\approx 20\%$) suggests that our error estimate is conservative.

5. RESULTS

The photometric and spectroscopic parameters for the elliptical galaxies in the clusters Abell 370 and MS 1512+36 at $z = 0.375$ are given in Table 2. Figure 2 shows the Mg_b-σ relation for the local comparison sample of Coma and Virgo ellipticals and the nine ellipticals observed in Abell 370 and MS 1512+36 at $z = 0.375$. The $z = 0.375$ objects show a Mg_b weakening of about 0.345 Å, which is typical for ellipticals at this redshift (Bender et al. 1996).

Figure 3 shows the edge-on view of the FP for Coma ellipticals with $\sigma > 120$ km s^{-1} and for the $z = 0.375$ ellipticals. The angular distances at which a perfect match between the two samples is achieved are 139 Mpc h_{50}^{-1} for Coma and 1400 Mpc h_{50}^{-1} for the $z = 0.375$ ellipticals (h_{50} is the Hubble constant in units of 50 km s^{-1} Mpc^{-1}); see below. The $z = 0.375$ objects are shown three times in Figure 3, first as observed in the rest-frame B band, then with a correction applied for cosmological $(1 + z)^4$ dimming, and finally corrected for luminosity evolution. The luminosity correction is calculated based on the *mean* offset in the Mg_b absorption of the local and the $z = 0.375$ sample, i.e., $\Delta \langle SB \rangle_{B,e} = 1.4 \Delta Mg_b = 0.48$ mag arcsec^{-2}. We could also have corrected the luminosity evolution of the objects individually and would have obtained the same result. In fact, the residuals of the distant ellipticals from the FP and from the Mg_b-σ relation correlate with each other in the expected way, although the error bars are large (see Fig. 4). This supports the idea that the evolution we see is really due to age. While for local samples of ellipticals we cannot conclude reliably that the residuals from the FP and Mg_b-σ relations are correlated and caused by age (see Jørgensen, Franx, & Kjærgaard 1996), the effects of age spread must
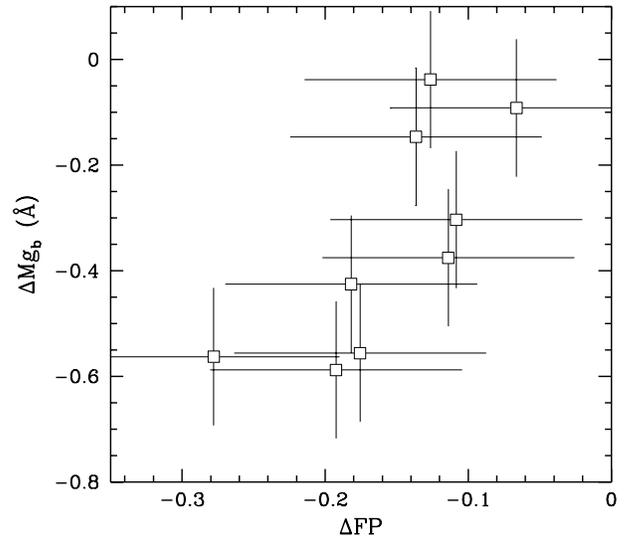

FIG. 4.—Residuals from the local fundamental plane vs. residuals from the local Mg_b-σ relation for the $z = 0.375$ ellipticals. Although the error bars are large, the residuals seem to correlate with each other.

increase with redshift and may lead to the correlation observed in Figure 4.

The cosmological model is constrained on the basis of Figure 3 as follows. The distance ratio at which the fully corrected FP of the $z = 0.375$ clusters matches the FP of Coma is 10.1 ± 0.8. With an angular distance of 139 Mpc h_{50}^{-1} for Coma (corrected to the cosmic microwave background rest frame following Faber et al. 1989), this ratio corresponds to an angular distance of 1400 Mpc h_{50}^{-1} for Abell 370 and MS 1512+36 at $z = 0.375$, which is the distance adopted in Figure 3 (h_{50} is the Hubble constant in units of 50 km s^{-1} Mpc^{-1}). For a plausible range of cosmological models, the distance to the Coma Cluster is, because of its proximity, virtually independent of q_0 (at the level of 0.5%), while the distance to the $z = 0.375$ clusters varies by more than 10%. Since the geometry of the universe is determined by the ratio of distances, q_0 is independent of the

TABLE 2

PHOTOMETRIC AND KINEMATIC DATA FOR ELLIPTICAL GALAXIES AT $z = 0.375$

Object Number	R_e (arcsec)	$\langle SB \rangle_e$ (B mag arcsec^{-2})	$\log R_e$ (kpc)	$\log \sigma$ (km s^{-1})	Mg_b (Å)
		Abell 370			
13	0.830	20.18	0.755	2.445	4.805
17	1.209	20.81	0.919	2.379	4.348
18	0.884	20.48	0.783	2.409	4.479
20	7.634	22.71	1.719	2.524	4.577
23	1.387	20.90	0.978	2.494	4.992
28	1.528	21.07	1.020	2.436	4.889
32	1.889	21.37	1.112	2.314	4.035
		MS 1512+36			
9	4.755	22.57	1.513	2.462	4.694
11	1.147	21.10	0.896	2.290	3.977

NOTE.—Object identification as in Ziegler & Bender 1997. Surface brightnesses are means within the effective radius, refer to the rest-frame B band, and are corrected for extinction and cosmological dimming but not for evolution. Effective radii in kiloparsecs were calculated with a distance of 1400 Mpc. Errors are given in Table 1 and shown in the plots.
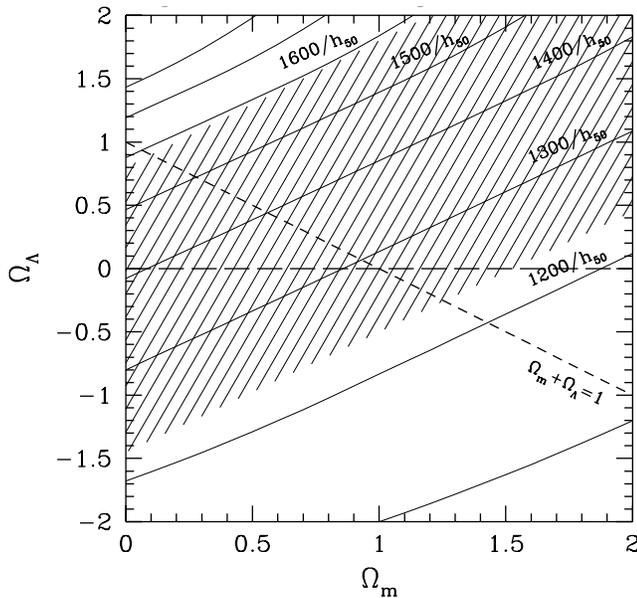
FIG. 5.—Plane of matter density as measured by Ω_m against Ω_Λ parameterizing the cosmological constant. Lines of constant angular distance for a redshift of 0.375 are shown. The ellipticals observed at this redshift allow us to constrain the angular distance to $z = 0.375$, which in turn defines a probability strip in the Ω_Λ-Ω_m plane. Values for Ω_Λ and Ω_m that have better than 90% likelihood lie in the shaded area. The horizontal long-dashed line corresponds to a universe without a cosmological constant, the diagonal short-dashed line to a universe with no curvature ($\Omega_m + \Omega_\Lambda = 1$).

ferred model would have $\Omega_m = \Omega_\Lambda = 0.5$. Ω_Λ is constrained to fall in the range $-0.25 < \Omega_\Lambda < +0.9$, again with 90% confidence.

6. CONCLUSIONS

We have explored the possibility of calibrating elliptical galaxies as cosmological standard rods. The proposed method is based on the fundamental plane relation of elliptical galaxies and the Mg_b-σ test, which allows us to calibrate the luminosity evolution of their stellar populations. The main assumptions that have to be made for this procedure to work are (1) that the fundamental plane and Mg-σ relations are the same for clusters of similar richness and (2) that the slope of the initial mass function of low-mass stars is known and has the same value in different objects and environments (here we adopt the Salpeter value). Further critical issues that need future checking are the reliability of stellar population models and the influence of sample selection effects and mixed populations.

A first application of the method has been given. We have shown that, with the provisos given above, it is possible to derive interesting constraints on the matter density and the cosmological constant using elliptical galaxies. In the future, stronger constraints should be possible if large samples of ellipticals up to redshift of close to 1 (Kelson et al. 1997) are analyzed in a similar way, and if the caveats and systematic effects discussed above can be controlled efficiently.

Hubble constant. The relative error of mean distance to the $z = 0.375$ clusters is about 8% (see Table 1). The mean distance to $z = 0.375$ and its error give immediate constraints on the cosmological model; see Figure 5. If the cosmological constant vanishes, then our measurements, together with the observational fact that there exists matter in the universe, constrain the cosmological density parameter to be $0 < \Omega_m < 1.4$, or the cosmological deceleration parameter to be $0 < q_0 < 0.7$, with 90% confidence. If the universe has flat geometry, as suggested by inflation, then the pre-

REFERENCES

Balogh, M. L., Morris, S. L., Yee, H. K. C., Carlberg, R. G., & Ellingson, E. 1997, ApJ, 488, L75
Bender, R. 1990, in Dynamics and Interactions of Galaxies, ed. R. Wielen (Heidelberg: Springer), 232
Bender, R., Burstein, D., & Faber, S. M. 1992, ApJ, 399, 462
———. 1993, ApJ, 411, 153
Bender, R., Ziegler, B., & Bruzual, G. 1996, ApJ, 463, L51
Bower, R., Lucey, J. R., & Ellis, R. S. 1992, MNRAS, 254, 601
Bressan, A., Chiosi, C., & Tantalo, R. 1996, A&A, 311, 971
Bruzual, G. A., & Charlot, S. 1998, in preparation
Burstein, D. 1989, in World of Galaxies, ed. H. G. J. Corwin & L. Bottinelli (New York: Springer), 547
Burstein, D., Faber, S. M., & Dressler, A. 1990, ApJ, 354, 18
Burstein, D., & Heiles, C. 1984, ApJS, 54, 33
Capelato, H. V., de Carvalho, R. R., & Carlberg, R. G. 1995, ApJ, 451, 525
Colless, M., et al. 1998, MNRAS, submitted
Djorgovski, S., & Davis, M. 1987, ApJ, 313, 59
Dressler, A., & Gunn, J. E. 1983, ApJ, 270, 7
Dressler, A., Lynden-Bell, D., Burstein, D., Davies, R. L., Faber, S. M., Terlevich, R. J., & Wegner, G. 1987, ApJ, 313, 42
Ellis, R. S., Smail, I., Dressler, A., Couch, W. J., Oemler, A., Butcher, H., & Sharples, R. 1997, ApJ, 483, 582
Faber, S. M., Dressler, A., Davies, R. L., Burstein, D., Lynden-Bell, D., Terlevich, R., & Wegner, G. 1987, in Nearly Normal Galaxies, from the Planck Time to the Present, ed. S. M. Faber (New York: Springer), 175
Faber, S. M., Wegner, G., Burstein, D., Davies, R. L., Dressler, A., Lynden-Bell, D., & Terlevich, R. J. 1989, ApJS, 69, 763

Glazebrook, K., Peacock, J. A., Miller, L., & Collins, C. A. 1995, MNRAS, 275, 169
Goobar, A., & Perlmutter, S. 1995, ApJ, 450, 14
Gorgas, J., Faber, S. M., Burstein, D., Gonzalez, J. J., Courteau, S., & Prosser, C. 1993, ApJS, 86, 153
Hamabe, M., & Kormendy, J. 1987, in IAU Symp. 127, Structure and Dynamics of Elliptical Galaxies, ed. T. de Zeeuw (Dordrecht: Reidel), 381
Jørgensen, I. 1997, MNRAS, 288, 161
Jørgensen, I., Franx, M., & Kjærgaard, P. 1995, MNRAS, 276, 1341
———. 1996, MNRAS, 280, 167
Kauffmann, G. 1996, MNRAS, 281, 487
Kelson, D. D., van Dokkum. P. G., Franx, M., Illingworth, G. D., & Fabricant, D. 1997, ApJ, 478, L13
Kormendy, J. 1977, ApJ, 218, 333
Leibundgut, B. 1996, ApJ, 466, L21
Lilly, S. J., Tresse, L., Hammer, F., Crampton, D., & Le Fèvre, O. 1995, ApJ, 455, 108
Linde, A. 1991, Phys. Scr., 36, 30
Longo, G., de Vaucouleurs, A., & Corwin, H. G. 1983, A General Catalogue of Photoelectric Magnitudes and Colors in the U, B, V System of 3,578 Galaxies Brighter than the 16th V-Magnitude (Austin: Univ. Texas)
Moore, B., Lake, G., & Katz, N. 1998 ApJ, in press (astro-ph/9701211)
Oemler, A., Dressler, A., & Butcher, H. 1997, ApJ, 474, 561
Perlmutter, S., et al. 1997, ApJ, 483, 565
Renzini, A., & Ciotti, L. 1993, ApJ, 416, L49

Saglia, R. P., Bender, R., & Dressler, A. 1993, A&A, 279, 75
Saglia, R. P., Bertschinger, E., Baggley, G., Burstein, D., Colless, M., Davies, R. L., McMahan, R. K., Jr., & Wegner, G. 1997a, ApJS, 109, 79
Saglia, R. P., Colless, M., Baggley, G., Bertschinger, E., Burstein, D., Davies, R. L., McMahan, R. K., Jr., & Wegner, G. 1997b, in Galaxy Scaling Relations: Origins, Evolution and Applications, ed. L. N. da Costa & A. Renzini (Heidelberg: Springer), 306
Sandage, A. 1995, in The Deep Universe, ed. A. Sandage et al. (Berlin: Springer)

Schweizer, F. 1990, in Dynamics and Interactions of Galaxies, ed. R. Wielen (Heidelberg: Springer), 60
Stanford, S. A., Eisenhardt, P. R. M., & Dickinson, M. 1998, ApJ, in press (astro-ph/970837)
van Dokkum, P. G., & Franx, M. 1996, MNRAS, 281, 985
Worthey, G. 1994, ApJS, 95, 107
Ziegler, B. L. 1998, in preparation
Ziegler, B. L., & Bender, R. 1997, MNRAS, 291, 527